UCRL-JC-124095
PREPRINT

CONF-961017--9

Lean-Burn Hydrogen Spark-Ignited Engines: The Mechanical Equivalent to the Fuel Cell

Salvador Aceves and J. Ray Smith

This paper was prepared for submittal to
American Society of Mechanical Engineers
Internal Combustion Engine
1996 Fall Conference
Fairborn, Ohio
October 20-23, 1996

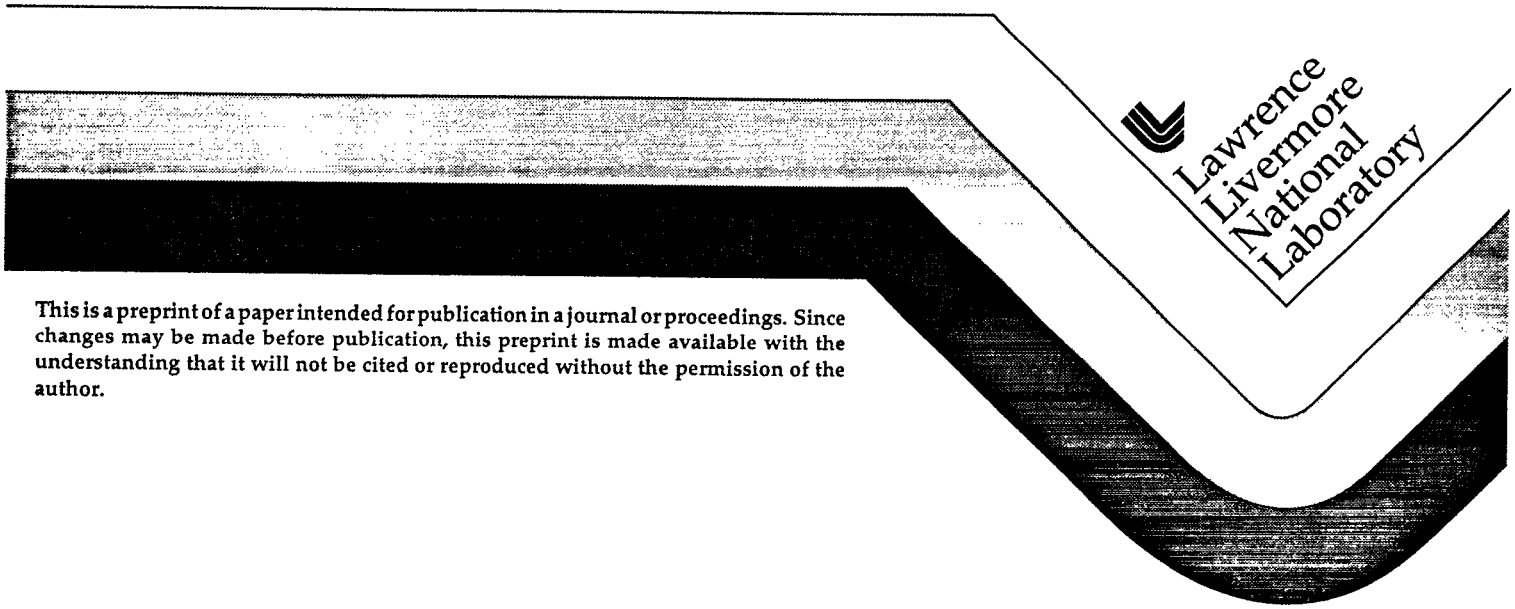

Lean-Burn Hydrogen Spark-Ignited Engines: The Mechanical Equivalent to the Fuel Cell*

by

Salvador M. Aceves and J. Ray Smith
Lawrence Livermore National Laboratory

Abstract

Fuel cells are considered as the ideal power source for future vehicles, due to their high efficiency and low emissions. However, extensive use of fuel cells in light-duty vehicles is likely to be years away, due to their high manufacturing cost.

Hydrogen-fueled, spark-ignited, homogeneous-charge engines offer a near-term alternative to fuel cells. Hydrogen in a spark-ignited engine can be burned at very low equivalence ratios, so that NO_x emissions can be reduced to less than 10 ppm without catalyst. HC and CO emissions may result from oxidation of engine oil, but by proper design are negligible (a few ppm). Lean operation also results in increased indicated efficiency due to the thermodynamic properties of the gaseous mixture contained in the cylinder. The high effective octane number of hydrogen allows the use of a high compression ratio, further increasing engine efficiency.

In this paper, a simplified engine model is used for predicting hydrogen engine efficiency and emissions. The model uses basic thermodynamic equations for the compression and expansion processes, along with an empirical correlation for heat transfer, to predict engine indicated efficiency. A friction correlation and a supercharger/turbocharger model are then used to calculate brake thermal efficiency. The model is validated with many experimental points obtained in a recent evaluation of a hydrogen research engine. The experimental data are used to adjust the empirical constants in the heat release rate and heat transfer correlation. The adjusted engine model predicts pressure traces, indicated efficiency and NO_x emissions with good accuracy over the range of speed, equivalence ratio and manifold pressure experimentally covered.

The validated model is applied to conditions that are considered to be of interest to vehicular applications in hybrids as well as conventional cars. It is recognized that using the engine model for conditions far from the experimental points may result in inaccuracies. Therefore, cylinder geometry is kept constant in the analysis, and only engine speed is varied beyond the range for which experimental data points are available. It is expected that such an extrapolation does not introduce large errors.

---

* Work performed under the auspices of the U.S. Department of Energy by the Lawrence Livermore National Laboratory under Contract No. W-7405-Eng-48.

The results present information that can be used to predict engine performance for vehicular applications, and are expected to serve as a first-order guide for engine sizing (number of cylinders) and control strategy selection. The results indicate that hydrogen lean-burn spark-ignited engines can provide Equivalent Zero Emission Vehicle (EZEV) levels in either a series hybrid or a conventional automobile.

Nomenclature

A	cylinder surface area
B	cylinder bore
C_1, C_2	constants in Equation 4.
h	heat transfer coefficient
n	shape parameter for burn fraction curve
p	pressure
q	heat transfer rate
S_p	mean piston speed
T	temperature
V	volume
w	gas velocity parameter
x	fraction of burn
θ	crank angle

Subscripts

d	displacement
m	motored
r	reference
w	wall

Introduction

Fuel cells have been recognized as the optimum power source for the light-duty fleet, due to their high efficiency and low (near zero) emissions (DeLuchi, 1992). Fuel cells provide the near-zero-emission benefits of electric vehicles, with the potential for long range and performance comparable to that of conventional cars. The major obstacles in the way of generalized use of vehicular fuel cells are their high cost, and the lack of an adequate fueling infrastructure. The need for a new fueling infrastructure can be reduced if a fuel reformer is installed onboard the vehicle, to convert a liquid fuel (e.g. methanol) to the high-purity hydrogen fuel required in PEM fuel cells (Appleby, 1993).

Hydrogen can also be used in spark-ignited piston engines. Hydrogen has very special properties, including a very high laminar flame speed, a high effective octane number, and no toxicity or ozone-forming potential (Smith, 1994). Homogeneous-charge spark-ignited piston engines can be designed to take advantage of these characteristics. The high laminar flame speed allows the use of very low equivalence ratios (as low as 0.2), reducing NO_x emissions to near-zero levels without requiring a catalytic converter, that may deteriorate with time. The use of low equivalence ratios also increases the indicated efficiency, and reduces the need for throttled operation (Heywood, 1988). The engine can have a high compression ratio, due to the high hydrogen octane number. Piston engines do not require a high-purity fuel, and can burn mixtures of hydrogen, carbon monoxide, and other gases.

Hydrogen piston engines can therefore be optimized to yield a high efficiency and near-zero emissions. While fuel cells have the potential for greater improvements in efficiency as well as emissions, piston engines are an inexpensive and well-known technology that can be applied in the short-term for obtaining basically the same benefits as fuel cell utilization.

This paper analyzes the applicability of hydrogen homogeneous-charge spark-ignited piston engines to Equivalent Zero Emission Vehicles (EZEV).[1] The analysis uses an engine model that is calibrated to match the data obtained in a recent experiment (Van Blarigan, 1996). The model is then used to generate engine performance maps for supercharged and turbocharged operation. These maps are applied for predicting fuel economy and emissions for conventional and series hybrid vehicles.

Experimental Engine Evaluation

The engine used in the experimental evaluation is an Onan engine which was modified by incorporating a head containing two spark plugs, along with the original two valves. The combustion chamber is a simple right circular cylinder with no squish and a flat top piston. This geometry has been shown to be the most efficient shape for reducing heat transfer losses in lean-burn engines (Olsson and Johansson, 1995). Engine characteristics are listed in Table 1, along with the range of conditions used in the experiment. The design of the Onan engine is based on the arguments set forth by Smith et al., 1995, to obtain a high efficiency, low emission engine. These guidelines include: extremely lean engine operation for high indicated efficiency and very low NO_x emissions; high compression ratio for high efficiency; long piston stroke, controlled turbulence, and big cylinders (low surface area to volume ratio) for reduced engine heat transfer losses; relatively low engine speed for reduced friction; and supercharged or turbocharged operation for improving specific power output and efficiency.

---

[1] Equivalent Zero Emission Vehicles are defined here as those that generate less emissions when operating inside the Los Angeles Basin than the power plant emissions generated as a result of electric car operation. These emission levels have been estimated as being one tenth of CARB ULEV standards, and are being considered for approval by CARB (CARB, 1995).

Figures 1 and 2 show the most important experimental results. Figure 1 shows indicated efficiency as a function of equivalence ratio, for all the experimental points at MBT timing obtained in the analysis. Engine speeds and supercharged operation are indicated with different symbols. A 0.39 equivalence ratio was selected for most supercharged runs. The figure shows that indicated efficiency increases as a function of engine speed, as a consequence of reduced heat transfer losses. The variation of indicated efficiency with equivalence ratio is best observed for 1200 rpm operation, for which the greatest fuel/air range was used. Indicated efficiency reaches a maximum near a 0.40 equivalence ratio. Increasing the equivalence ratio from this point results in a decreased indicated efficiency, due to a decreased specific heat ratio ($\gamma=c_p/c_v$) for the gas inside the cylinder (Heywood, 1988). Decreasing the equivalence ratio from the optimum point increases the timing losses, due to slower heat release, thereby reducing the indicated efficiency. Supercharged operation results in small indicated efficiency gains due to slightly lower heat transfer losses per unit mass of fuel at the higher densities. Supercharged operation has a larger effect on brake thermal efficiency by increasing the output work relative to the frictional work.

Figure 2 shows NO_x emissions as a function of equivalence ratio. The figure shows that NO_x emissions are very insensitive to engine speed and supercharged operation, and correlate very well with equivalence ratio. It is concluded that the modified Zeldovich mechanism (Heywood, 1988) describes NO_x production well. Spatial simulations using a 2-dimensional version of KIVA (Amsden, 1993) indicate that 80% of the NOx is produced by the first 20% of the burned gas when the last-burned gas recompresses the first-burned gas.

Engine Model

The engine model uses first principles and correlations to predict piston engine efficiency and power output. The engine model is a lumped (zero-dimensional), time-dependent model which solves the basic differential equations for the compression and power strokes. The following empirical expression is specified for the shape of the heat release curve (Ferguson, 1986):

$$x = x_{max}\left[1 - \exp\left(\frac{\theta - \theta_s}{\theta_b}\right)^n\right] \qquad (1)$$

where θ is the instantaneous crank angle, θ_s is the ignition angle, and θ_b and n are shape parameters for the resultant "s" curve. The values of θ_s, θ_b, and n are determined for each experimental run by using an optimizer (Haney et al., 1992) to find the combination of the three parameters that minimizes the differences between the experimental pressure trace and the pressure trace calculated by the model. The results have been very satisfactory.

The relative errors in matching the pressure traces have been of the order of 0.5%, with a maximum error of 1% over all engine speeds, equivalence ratios and manifold pressures. The ranges for θ_b and n are: $15° \leq \theta_b \leq 30°$ and $1.15 \leq n \leq 1.45$.

The engine model uses Woschni's correlation (Woschni, 1967) to estimate engine heat transfer. This correlation is given as:

$$q = h\,A\,(T - T_w) \tag{2}$$

with

$$h = 3.26\,B^{-0.2}\,p^{0.8}\,T^{-0.55}\,w^{0.8} \tag{3}$$

where q is the overall heat transfer rate, A is the cylinder area, h is the heat transfer coefficient in W/m^2K, B is the cylinder bore in m, p is the pressure in kPa, T is the mass-averaged temperature in K, and w is a measure of the gas velocity inside the cylinder, given as:

$$w = C_1\,S_p + C_2\,V_d\,T_r\,(p-p_m)/p_r\,V_r \tag{4}$$

Where $C_1 = 2.28$ during the compression and expansion periods; S_p is the mean piston speed; $C_2 = 0.00324$; V_d is the displaced volume; T_r, p_r and V_r are temperature, pressure and volume at a reference state; and $p-p_m$ is the difference between the cylinder pressure and the motored pressure. The variables are a function of time, and are calculated for each crank angle degree of engine rotation. It was found during the analysis that the heat transfer correlation underpredicts heat transfer losses. Therefore, the original values of the constants C_1 and C_2 given above were multiplied by 1.8, resulting in a better match with the experimental data.

The engine model includes a friction model and a supercharger/turbocharger model to predict brake thermal efficiency. The friction model uses a detailed correlation developed by Patton et al., 1989. Supercharger and turbocharger performance is calculated by using a thermodynamic model and assuming a constant (0.7) isentropic efficiency for both the turbine and the compressor. Selection of a supercharger to match the energy control demands is outside the current experience of the authors. However, a detailed supercharger map could be incorporated into the model if further refinement is desired. A water-cooled intercooler is assumed with a thermal effectiveness of 0.7. A model for NO_x emissions prediction is incorporated in the engine model. Emissions of NO_x are calculated as a function of engine equivalence ratio (Figure 2). A correction is used for supercharged and turbocharged operation, to take into account the higher intake temperature resulting from the compression process and the less than perfect effectiveness of the intercooler. Based on reported data for typical engines (Heywood, 1988), volumetric efficiency is assumed to vary from 85% at low engine speeds, to a maximum of 95% at 4000 rpm, down to 90% at 5000 rpm.

The engine model is validated by comparing the calculated and experimental indicated efficiencies. Figure 3 shows experimental (from Figure 1) and model results as a function of equivalence ratio. The figure indicates that the model predicts absolute values as well as trends with good accuracy for engine indicated efficiency, over the whole range of operating conditions, with the maximum error of the order of 1%. NO_x emissions are also predicted to within a good approximation with the correlation of NO_x as a function of equivalence ratio. No validation is done for brake thermal efficiency, because the Onan engine used in the experiment has substantially more friction per cylinder than a current automotive engine, for which Patton's correlation applies.

The engine model is then applied to predicting the engine and vehicle performance that result if a 4-cylinder (1.97 liter) hydrogen engine is built with the same cylinder characteristics of the Onan engine. The geometry of the engine cylinders is not changed in the analysis, because small changes in geometry may result in significant changes in efficiency. It is expected, however, that larger engine cylinders will improve engine efficiency.

Using the engine model for predicting vehicle performance requires extrapolating from the engine speeds used in the experiment (1200-1800 rpm) to engine speeds that are required for vehicle operation. A maximum engine speed of 5000 rpm is assumed. It is recognized that this extrapolation may result in errors. Errors are due to turbulence variations with engine speed which influence heat release rate, thus changing both timing losses and heat transfer losses. However, Figure 3 shows that the model predicts the efficiency trends with good accuracy for the range in which experimental data exist, and it is considered that the model can do a reasonable job at predicting efficiency for high engine speeds. In addition to this, engines in conventional and series hybrid vehicles are most often operated at low to moderate speeds, which is the range for which the model has been validated. For the conventional vehicle analyzed in a later section of this paper the mean engine speed is 1500 rpm for the urban cycle and 2700 rpm for the highway cycle. Maximum engine speed for the driving cycles is 3300 rpm. The series hybrid vehicle is set to operate at a constant 2400 rpm during the driving cycles.

Engine brake thermal efficiencies are required for applying the engine code to vehicle calculations, and brake thermal efficiencies are calculated with a friction and a supercharger/turbocharger model that have not been validated for this particular application. While the model cannot replace experimental runs, it is considered that the brake thermal efficiencies calculated with the model give a good idea of the performance that can be obtained with such an engine. Engine emissions are very insensitive to engine operating conditions other than maximum temperature within the cylinder (Figure 2), and it is therefore expected that the engine NO_x model can provide accurate predictions for emissions levels throughout the operating range.

The engine model is applied to generate engine emissions and performance maps, necessary for predicting vehicle performance. A conventional engine has only one degree of freedom for controlling the output torque at any given speed: the inlet manifold

pressure. This is due to the use of three-way catalysts that require near-stoichiometric operation for high conversion efficiency. A hydrogen engine has two degrees of freedom, because equivalence ratio can also be varied. Generating an engine map therefore requires determining a control strategy that specifies how to adjust these two parameters to obtain the desired torque for any given engine speed. In this analysis, an optimizer (Haney et al., 1992) is used to determine the combination of equivalence ratio and inlet manifold pressure that satisfies the torque requirement while providing the maximum engine brake thermal efficiency. A constraint is used in the optimization: engine NO_x emissions are less than 10 ppm under all operating conditions. An engine generating 10 ppm of NO_x is well below the EZEV standards, provided that it is installed in a vehicle with a fuel economy of 40 mpg or higher.

Lean operation results in low power output, and therefore turbocharged or supercharged operation is required for providing a reasonably high power output. Both supercharged and turbocharged operation have been considered for generating the engine performance map. The performance maps for both cases are very similar, with turbocharged operation having a slight efficiency advantage over supercharged operation. Only the results for supercharged operation are shown in this paper. Supercharged operation is preferred to turbocharged operation due to the lag time that may exist in turbocharged operation.

Results

Figures 4-7 show the predictions for engine efficiency and emissions maps, as well as the optimum control strategy for inlet equivalence ratio and pressure, for the 4-cylinder supercharged engine.

Figure 4 shows lines of constant brake thermal efficiency (in percent) as a function of engine speed and engine torque. The figure also shows a dotted line corresponding to the conditions at which the engine generates 10 ppm of NO_x. This restriction sets the limit on the maximum torque and power that can be obtained from the engine. Maximum power approaches 60 kW at 5000 rpm. The contour lines in this and the following figures spread beyond the 10 ppm line, to show the potential power gains obtained with relaxing this restriction. A square in the figure indicates the approximate range of experimental conditions covered.

Figure 4 shows that the engine is predicted to have a broad area of high efficiency, for intermediate speeds and high torques. The efficiency drops for lower speeds due to increased heat transfer losses, and for higher speeds due to increased friction. As expected, the efficiency drops to zero as the load is reduced. However, the drop occurs more slowly than in conventional engines, because the equivalence ratio can be reduced as the load is reduced, resulting in lower throttling losses.

Figure 5 shows contours of NO_x emissions in ppm as a function of engine speed and torque. Engine levels are near zero (<2 ppm) over the low load range, which is the range at which the engine is operated most of the time during city and highway driving in conventional cars. Emissions increase slowly as the torque increases, until the restriction of 10 ppm is approached. When this restriction is approached, the operating conditions in the engine are adjusted so that the 10 ppm line is pushed as high as possible by increasing the manifold pressure without further increases in equivalence ratio, at the cost of some losses in efficiency. This explains the great distance between the 8 ppm and the 10 ppm shown in the figure. Emission levels shown in the figure are expected to be valid over the lifetime of the engine, since no catalytic converter is used to control emissions. Emission levels are only a function of equivalence ratio and manifold pressure, and are therefore not expected to increase with use, as occurs in gasoline engines due to catalytic converter deterioration.

Figure 6 shows contour lines of equivalence ratio as a function of engine speed and torque. Equivalence ratios shown in the figure are optimum values, that result in the maximum possible brake thermal efficiency, while meeting the 10 ppm NO_x limit. The figure includes a dotted line for the 10 ppm NO_x limit. Figure 6 shows that engine equivalence ratio is reduced down to 0.24 at the low load conditions, to reduce throttling losses. Equivalence ratio is then increased as the torque is increased, until the 10 ppm NO_x limit is approached. At this point, equivalence ratio cannot be increased any further, and additional power is obtained by supercharging (Figure 7). Equivalence ratio has to be reduced as the inlet pressure increases, to compensate for the higher temperature of the intake gases. The reduction of equivalence ratio with increasing torque appears in the figure as sharp corners in the equivalence ratio lines at about 80 Nm.

Figure 7 shows contour lines of optimum inlet pressure (in bars) as a function of engine speed and torque. Pressures in the figure are selected to provide the maximum possible brake thermal efficiency, while meeting the 10 ppm NO_x limit. The figure includes a dotted line for the 10 ppm NO_x limit. Inlet pressure is kept relatively high (0.5 bar) at the very low load conditions to reduce throttling losses. The engine operates without supercharging over most of the low-load conditions that are required for typical urban and highway driving. When the 10 ppm NO_x limit is approached, pressure is increased rapidly to provide the required power without increasing equivalence ratio (which would increase combustion temperature and therefore NO_x). The maximum NO_x curve limits the maximum supercharge pressure to about 2 bar at the low speed limit, although the maximum pressure is 1.8 bar over most of the engine speed range.

Application to Conventional and Series Hybrid Vehicles

The engine efficiency and NO_x maps presented in the previous section are now used in predicting vehicle fuel economy, performance and emissions for a conventional and a series hybrid vehicle. This is accomplished by incorporating the engine maps into an

existing vehicle evaluation code (Aceves and Smith, 1995). The main characteristics of the two vehicles are listed in Table 2. Both vehicles have a low weight, with the series hybrid vehicle weighing 100 kg more than the conventional car, due to the additional components required in the series hybrid power train. The engine and the hydrogen storage tank for the series hybrid vehicle can be downsized to reduce the weight differential between the two cars. This possibility, however, is not considered in this analysis. It is assumed that liquid hydrogen cryogenic storage is used, since hydride storage would result in a substantially increased vehicle weight. Liquid hydrogen storage also has a reasonable volume (about 110 liters, 30 gallons, for 5 kg of hydrogen), compared with the volume required for compressed hydrogen (about 220 liters, 60 gallons, at 34 MPa, 5000 psi). The conventional engine has a 5-speed transmission, and the series hybrid a single-speed transmission. Both transmissions have been optimized by finding the reduction ratios (and shift points for the conventional car) that result in maximum vehicle efficiency The series hybrid car uses a high efficiency flywheel (Post et al., 1993), a permanent magnet generator, and an induction motor.

Conversion between ppm of NO_x, obtained from the engine maps, and grams per km (mile), specified in the emissions regulations, requires a knowledge of the composition of NO_x (fraction of NO and NO_2 in the mixture). It was found in the experiment that NO_2 emissions are a significant part of the total NO_x emissions, due to the very low equivalence ratios used. The calculation of grams/km of NO_x done in this analysis assumes that half of the NO_x produced per unit volume is NO_2. This is a conservative assumption, since NO_2 emission levels are lower over most operating conditions.

Table 3 shows the results of the analysis. Fuel economy is given as gasoline-equivalent energy consumption. The conventional vehicle has a reasonably high fuel economy (17.4 km, 41 mpg). The vehicle range (330 km, 205 miles) is lower than obtained in gasoline vehicles, but is still high enough to not represent a limitation on the applicability of the vehicle to most circumstances. The conventional vehicle has reasonable acceleration and hill climbing performance. The most desirable feature of the conventional car is the emission levels. Emissions are projected to be a factor of 75 lower than the CARB ULEV requirements, and therefore a factor of 7.5 lower than EZEV. The reason for the emissions to be so low is that the engine is operated most of the time at low torque, generating much less than the 10 ppm maximum allowable NO_x (Figure 5). Using the 10 ppm NO_x restriction guarantees that any driver obtains EZEV emissions, regardless of how aggressively they may drive.

The four cylinder engine has also been optimized considering a 100 ppm maximum NO_x, to observe how this change affects vehicle performance and emissions. It is found that changing the maximum NO_x limit causes very little change in driving cycle emissions and fuel economy, because the urban and highway cycles are driven at low torque conditions, for which the NO_x limit does not have an effect. The major difference is an increase in the maximum engine power, from 60 kW to 75 kW, which results in a significant gain in performance (the time for 0 to 97 km/hr acceleration drops to 7.9 s, and the maximum continuous slope at 97 km/h increases to 16%). However, an aggressive driver may

operate the vehicle at conditions that result in NO_x emissions that do not meet the EZEV limits.

The series hybrid vehicle has a very high fuel economy (26.9 km/l, 63.2 mpg), a range similar to conventional gasoline vehicles (508 km, 316 miles) and reasonable performance. Emissions are higher than for conventional cars, but still within EZEV limits. Emissions are higher than for conventional cars because the engine in a series hybrid vehicle operates at or near maximum efficiency, to maximize fuel economy. In this case, maximum engine efficiency (36%) is obtained near the 10 ppm emission limit (Figures 4 and 5).

Fuel economy projected for the series hybrid engine vehicle is low compared to the 33.5 km/l (79 mpg) predicted for a hydrogen series hybrid vehicle in a previous work by the authors (Aceves and Smith, 1995). The results are different because the engine model used in this analysis is based on experimental data for a particular engine (Onan), while the previous work indicates improvements that are likely to be obtained in a future optimized hydrogen engine.

Conclusions

This paper presents the development and validation of a simplified (zero-dimensional) engine model. The model is applied to a hydrogen engine which has been experimentally tested. The model predicts accurately engine efficiency and NO_x emissions over the full range of operating conditions. The validated model is then used to generate engine performance and emission maps for supercharged engine operation. The performance maps are then incorporated into a vehicle evaluation code to obtain performance and emissions for hydrogen-fueled conventional and series hybrid vehicles. Analysis of these two vehicles yields the following results:

1. The conventional vehicle has a high fuel economy, reasonable acceleration and hill climbing performance and a short but acceptable range. Emissions out of the conventional car are projected to be a factor of 75 lower than the CARB ULEV requirements, and therefore a factor of 7.5 lower than EZEV. The engine control strategy presented in this paper guarantees that the conventional vehicle achieves EZEV emissions levels regardless of how the car is driven.

2. The series hybrid vehicle has a very high fuel economy, a range similar to conventional gasoline vehicles, and reasonable performance. Emissions are higher than for conventional cars, but still within EZEV limits. Emissions in a series hybrid vehicle are intrinsically independent of driver's input.

These results indicate that lean-burn hydrogen spark-ignited engines provide basically the same benefits as a fuel cell, with a technology that is well-known and can be applied

immediately. Emission control is achieved without a catalytic converter, and emission levels are therefore not expected to deteriorate with time.

References

1. Aceves, S.M., and Smith, J.R., 1995, "A Hybrid Vehicle Evaluation Code and Its Application to Vehicle Design," SAE paper 950491.

2. Amsden, A.A., 1993, "KIVA-3, A KIVA Program with Block-Structured Mesh for Complex Geometries," Los Alamos National Laboratory Report LA-12503-MS.

3. Appleby, A.J., 1994, "Fuel Cells and Hydrogen Fuel," International Journal of Hydrogen Energy, Vol. 19, pp. 175-180.

4. California Air Resources Board, Mobile Sources Division, 1995, "Proposed Ammendments to the Low-Emission Vehicle Regulations to Add an Equivalent Zero-Emission Vehicle (EZEV) Standard and Allow Zero-Emission Vehicle Credit for Hybrid Electric Vehicles," Preliminary Draft Staff Report, CARB, El Monte, CA, July 14.

5. DeLuchi, M., 1992, "Hydrogen Fuel Cell Vehicles," University of California Davis Institute of Transportation Studies Report UCD-ITS-RR-92-14.

6. Ferguson, C.R., 1986, "Internal Combustion Engines, Applied Termosciences," John Wiley and Sons, New York.

7. Haney, S.W., Barr, W.L., Crotinger, J.A., Perkins, L.J., Solomon, C.J., Chaniotakis, E.A., Freidberg, J.P., Wei, J., Galambos, J.D., and Mandrekas, J., 1992, "A SUPERCODE for Systems Analysis of Tokamak Experiments and Reactors," Fusion Technology, Vol. 21, p. 1749.

8. Heywood, J.B., 1988, Internal Combustion Engine Fundamentals, McGraw-Hill, New York.

9. Olsson K., and Johansson, B., 1995, "Combustion Chambers for National Gas SI Engines Part 2: Combustion and Emissions," SAE paper 950517.

10. Patton, K.J., Nitschke, R.G., and Heywood, J.B., 1989, "Development and Evaluation of a Friction Model for Spark-Ignition Engines," SAE Paper 890836.

11. Post, R.F., Fowler, T.K., and Post, S.F., 1993, "A High-Efficiency Electromechanical Battery," Proceedings of the IEEE, Vol. 81, pp. 462-474.

12. Smith, J.R., 1994, "Optimized Hydrogen Piston Engines," Proceedings of the 1994 International Congress on Transportation Electronics, Convergence 1994, SAE, pp. 161-166.

13. Smith, J.R., Aceves, S.M., and Van Blarigan, P., 1995, "Series Hybrid Vehicles and Optimized Hydrogen Engine Design," SAE Paper 951955.

14. Van Blarigan, P., 1996, "Development of a Hydrogen-Fueled Internal Combustion Engine Designed for Single Speed/Power Operation," Submitted to the 1996 SAE Future Transportation technology Conference and Exposition, Vancouver, BC.

15. Woschni, G., 1967, "Universally Applicable Equation for the Instantaneous Heat Transfer Coefficient in the Internal Combustion Engine," SAE Paper 670931.

Table 1. Modified Onan engine characteristics and experimental conditions.

Bore, mm	82.55
Stroke, mm	92.08
Displacement, cm^3	493.0
Geometric compression ratio	14.0
Experimental range for equivalence ratio	0.2-0.5
Experimental range for engine speed, rpm	1200-1800
Experimental range for volumetric efficiency, %	90-215

Table 2. Main parameters for hydrogen-fueled conventional and series hybrid vehicles.

Vehicle parameter	conventional	series hybrid
test weight, kg (empty wt. + 136 kg)	1136	1236
frontal area, m^2	2.04	2.04
aerodynamic drag coefficient	0.24	0.24
coefficient of rolling friction	0.007	0.007
transmission efficiency	0.94	0.95
transmission gears	5	1
accessory load, W	1000	1000
hydrogen storage capacity, kg	5	5
engine idling speed, rpm	600	-
launch engine RPM, maximum effort acceleration	3600	-
regenerative braking	no	yes
generator type	-	permanent magnet
motor type	-	AC induction
energy storage device	-	flywheel
motor maximum torque, Nm	-	95
motor maximum speed, rpm	-	11000
flywheel energy storage, kWh	-	1
flywheel maximum power, kW	-	100

Table 3. Performance and emissions results for the conventional and series hybrid hydrogen-fueled vehicles.

Vehicle parameter	conventional	series hybrid
fuel economy[1], urban cycle, km/liter (mpg)	15.0 (35.3)	24.7 (58.2)
fuel economy[1], highway cycle, km/liter (mpg)	21.7 (51.1)	30.0 (70.6)
fuel economy[1], combined cycle, km/liter (mpg)	17.4 (41.0)	26.9 (63.2)
NO_x emissions, urban cycle, g/km (g/mile)	0.0020 (0.0032)	0.012 (0.019)
NO_x emissions, highway cycle, g/km (g/mile)	0.0013 (0.0020)	0.0097 (0.015)
NO_x emissions, combined cycle, g/km (g/mile)	0.0016 (0.0027)	0.011 (0.018)
time for 0-97 km/h (0-60 mph), s	10.0	10.0
maximum climbing slope at 97 km/h (60 mph), %	13.1	6.0
vehicle range, combined cycle, km (miles)	330 (205)	508 (316)

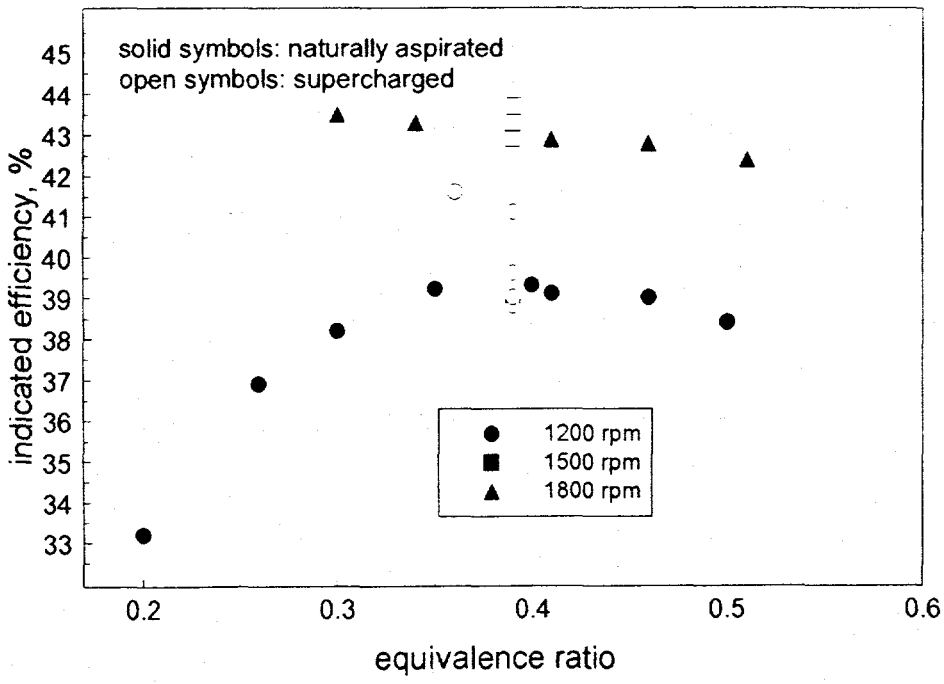

Figure 1. Indicated efficiency for the Onan engine as a function of equivalence ratio, for all the experimental points at MBT timing obtained in the analysis. Engine speeds and supercharged operation are indicated with different symbols.

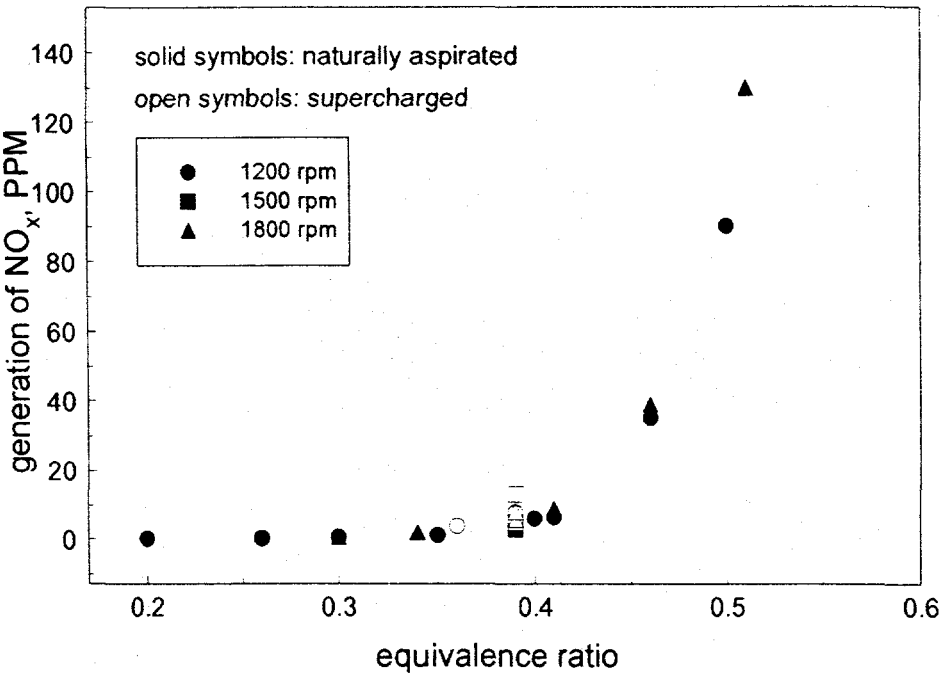

Figure 2. Emission of NO_x in parts per million for the Onan engine as a function of equivalence ratio, for all the experimental points at MBT timing obtained in the analysis. Engine speeds and supercharged operation are indicated with different symbols.

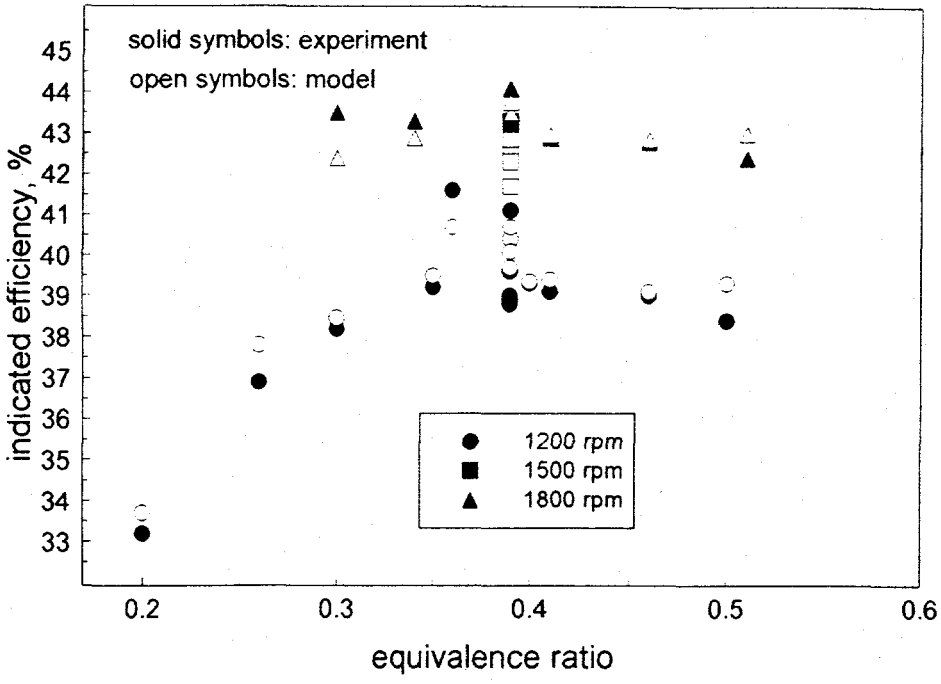

Figure 3. Indicated efficiency for the Onan engine as a function of equivalence ratio. The figure includes both the experimental results and the model predictions.

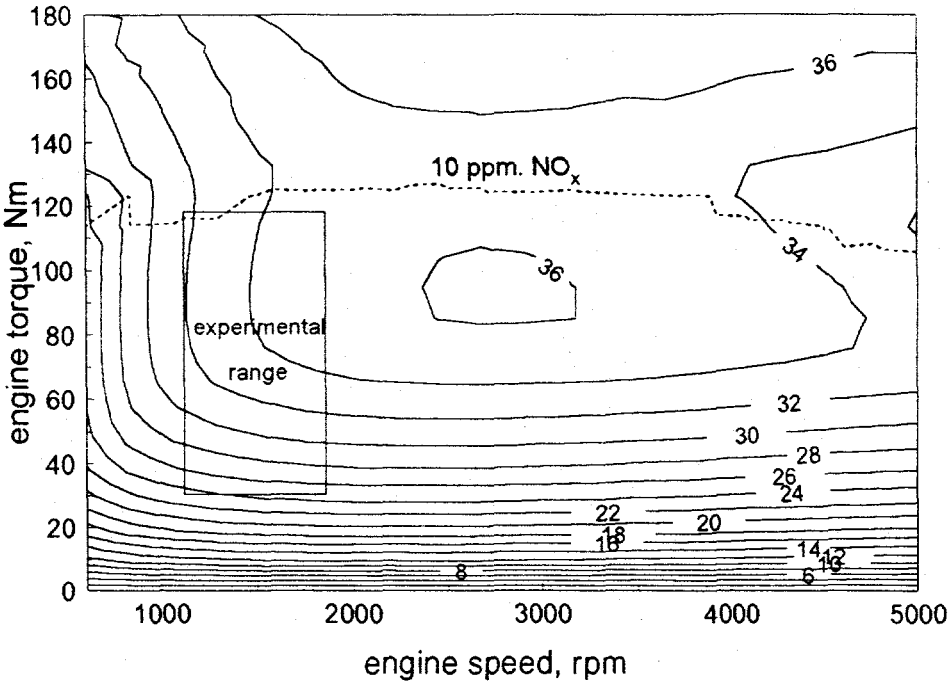

Figure 4. Contour lines of constant brake thermal efficiency (in percent) as a function of engine speed and engine torque. The dotted line corresponds to the conditions at which the engine generates 10 ppm of NO_x, and the square indicates the approximate area in which the experimental data were taken.

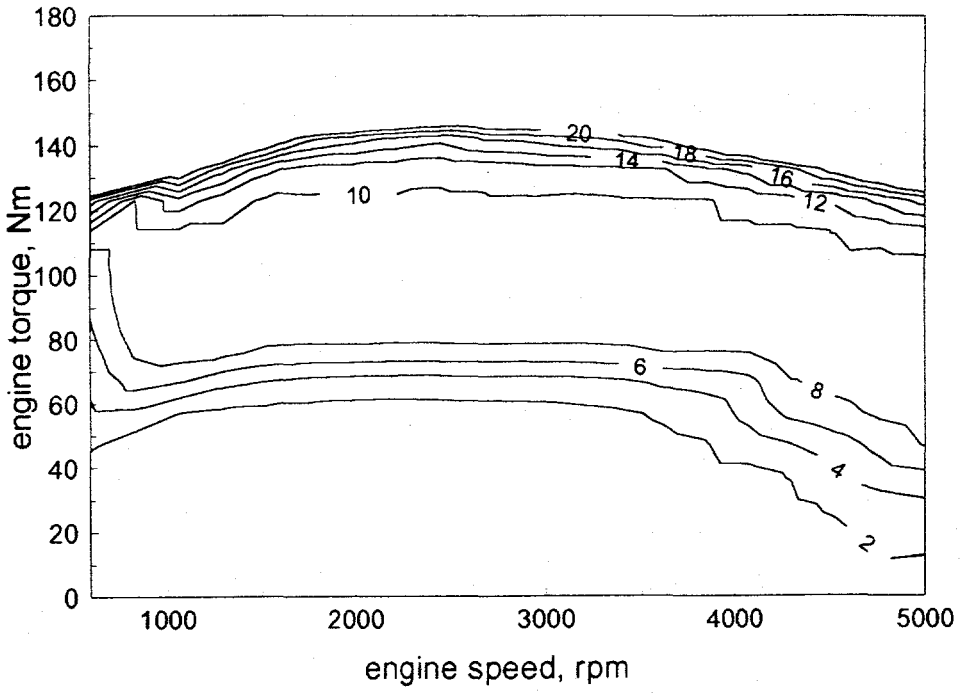

Figure 5. Contours of NO_x emissions in ppm as a function of engine speed and torque, for the optimized hydrogen engine.

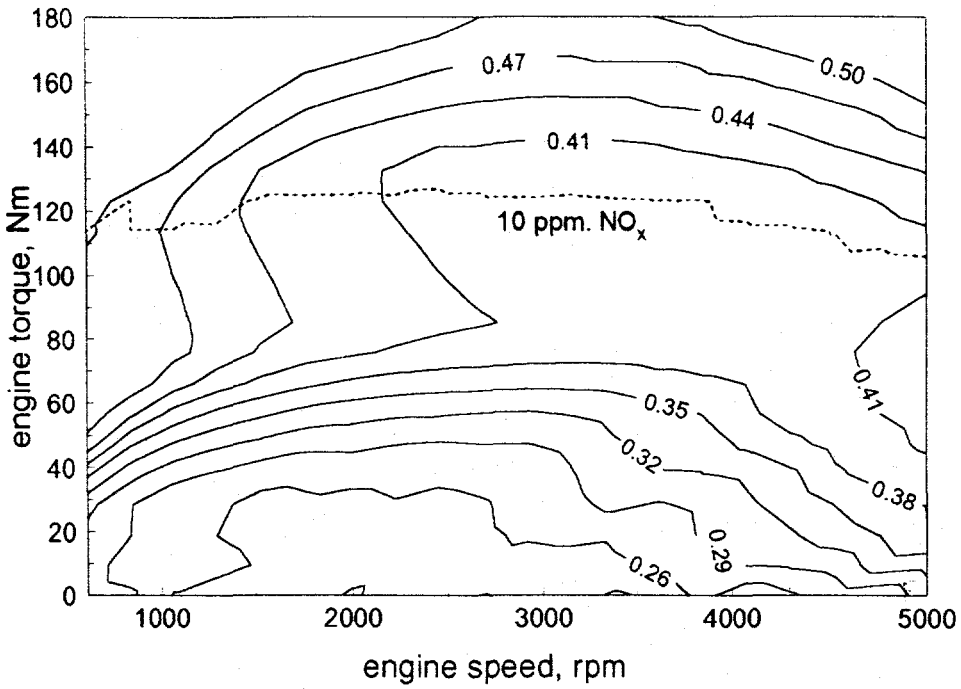

Figure 6. Contour lines of equivalence ratio as a function of engine speed and torque. Equivalence ratios shown in the figure are optimum values, that result in the maximum possible brake thermal efficiency, while meeting the 10 ppm NO_x limit. The figure includes a dotted line for the 10 ppm NO_x limit.

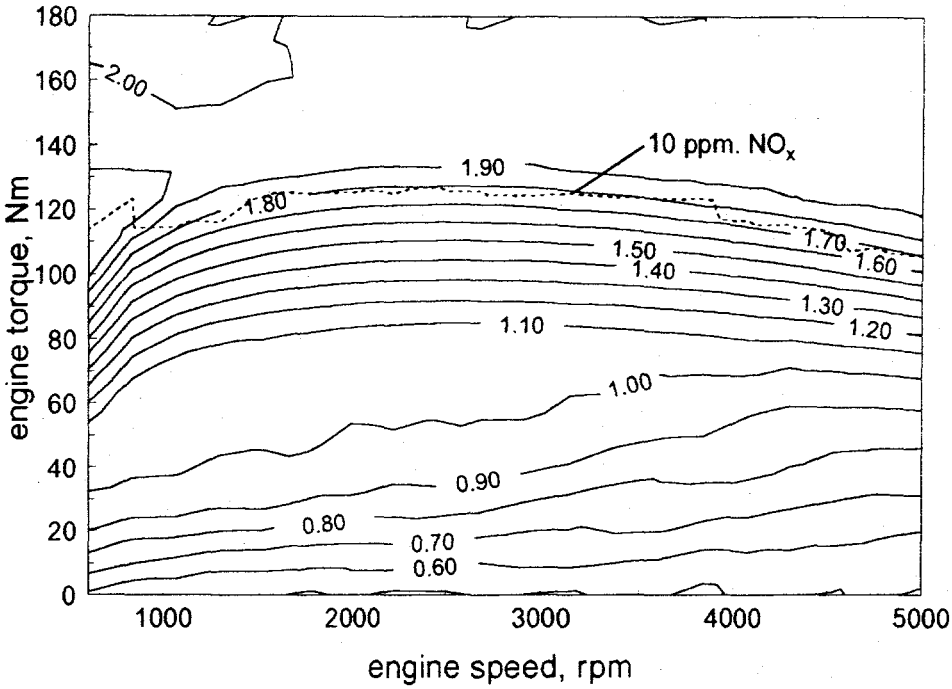

Figure 7. Contour lines of optimum inlet pressure (in bars) as a function of engine speed and torque. Pressures in the figure are selected to provide the maximum possible brake thermal efficiency, while meeting the 10 ppm NO_x limit. The figure includes a dotted line for the 10 ppm NO_x limit.